JOURNAL OF GUIDANCE, CONTROL, AND DYNAMICS
Vol. 34, No. 3, May–June 2011

Time-of-Arrival Taxi Conformance Monitoring for Surface Operations

Qian Zheng* and Yiyuan J. Zhao†
University of Minnesota, Minneapolis, Minnesota 55455
and
Brian Capozzi‡
Mosaic ATM, Inc., Leesburg, Virginia 20175

DOI: 10.2514/1.52047

This paper presents a systematic procedure and required algorithms for time-of-arrival taxi conformance monitoring in air traffic surface operations. Time-of-arrival taxi conformance monitoring determines if an aircraft is able to pass or arrive at specified checkpoints on a taxi route on time. The proposed procedure is first based on predicting times of arrival at a checkpoint. Two different time-of-arrival prediction methods are presented. The dead-reckoning method assumes that the aircraft maintain a constant speed in the near future. In comparison, the intent modeling method assumes a dynamic speed profile that consists of a series of different segments. In each segment, the aircraft may accelerate, decelerate, or maintain a constant speed. Both the taxi route geometry and aircraft performance capabilities are used in establishing the natures and magnitudes of these segments. Next, a taxi conformance monitoring criterion is introduced that takes into consideration the range of feasible aircraft times of arrival at the checkpoint, or time controllability. It takes as inputs current measured aircraft states, aircraft speed limits, its maximum acceleration and deceleration capabilities, and distance to the checkpoint. Human-in-the-loop simulation traffic data from the Dallas–Fort Worth airport is used and Monte Carlo simulations are conducted over likely uncertainties of aircraft state measurements to evaluate the proposed methods in terms of time-of-arrival prediction accuracy, speed profile matching, and conformance prediction reliability.

Nomenclature

$a_{\max}$	=	maximum acceleration rate
d	=	relative distance
$d_{\max}$	=	maximum deceleration rate
g	=	gravitational acceleration
I	=	conformance metric
R	=	checkpoint
s	=	position along the route
s_R	=	position of checkpoint R
$\hat{s}_i$	=	estimated position at time t_i
t_R	=	required time of arrival at checkpoint R
$\hat{t}_R^i$	=	time of arrival at checkpoint R predicted at time t_i
$\hat{t}_{R\max}^i$	=	maximum time of arrival at checkpoint R predicted at time t_i
$\hat{t}_{R\min}^i$	=	minimum time of arrival at checkpoint R predicted at time t_i
t	=	time
t_i	=	time at the current position
t_0	=	initial time
V	=	ground speed
$\dot{V}$	=	acceleration
V_c	=	commanded speed
$\hat{V}_i$	=	estimated current speed
$V_{\max}$	=	maximum speed
$V_{\min}$	=	minimum speed
V^-	=	speed between $V_{\min}$ and V_c
V^+	=	speed between V_c and $V_{\max}$
x, y	=	east, north position
Δt_R	=	time-of-arrival tolerance
ϵ	=	small positive number

Presented as Paper 2010-7544 at the AIAA Guidance, Navigation, and Control Conference, Toronto, Canada, 1–5 August 2010; received 19 August 2010; revision received 12 January 2011; accepted for publication 27 January 2011.

*Research Associate, Department of Aerospace Engineering and Mechanics; qzheng@aem.umn.edu.
†Professor, Department of Aerospace Engineering and Mechanics; gyyz@aem.umn.edu. Associate Fellow AIAA.
‡Principal Analyst; bcapozzi@mosaicatm.com. Member AIAA.

I. Introduction

HISTORICALLY, a large portion of aircraft flight delays are incurred during surface operations. Indeed, airport capacity constraint represents one of the biggest challenges to accommodating the increased traffic as envisioned in the Next Generation Air Transportation System (NextGen) [1]. Therefore, it is highly desirable to develop computer automation tools to enable maximum throughput and capacity in the airport environment.

Research activities in the Safe and Efficient Surface Operations (SESO) [2–4] project investigate new technologies and concepts to increase airport capacity by enhancing the flexibility and efficiency of surface operations. In particular, SESO research on integrated surface operations scheduling seeks to generate robust optimized solutions for surface traffic planning and control to improve surface throughput with little or no increase in delays. They do so by properly selecting spot/gate release times, taxi routes, and runway schedules for both departing and arriving aircraft, subject to appropriate requirements on minimum separation, aircraft speed limits, and active runway crossing. The required times of arrival (RTA) at designated traffic flow points or checkpoints and/or the corresponding speed profiles become commands for pilots to follow in implementing these schedules [5,6].

In practical operations, it is vitally important that individual aircraft closely adhere to optimized RTA schedules if their full benefits in maximizing the efficiency and throughput are to be realized. In fact, any significant deviations from these schedules may even cause the loss of sufficient interaircraft separations. As a result, taxi conformance monitoring systems are needed that can timely detect any potential deviations from planned taxi schedules, so that advance warnings can be issued to pilots and/or controllers for proper corrective maneuvers.

Aircraft conformances to planned taxi schedules may be divided into taxi route conformance and time-of-arrival (TOA) conformance. An aircraft conforms to the planned taxi route if it moves along the prescribed route. A nonconformance to the planned route can be detected by estimating aircraft current and future positions, and then comparing these estimates with the coordinates of planned routes. In comparison, TOA based taxi conformance monitoring seeks to determine if an aircraft will be able to timely pass or arrive at a specified checkpoint on a specified route or it will be either ahead of or behind the RTA beyond a tolerance margin. In the latter case, the system would estimate the likelihood of the excursion, and the likely first instant at which this excursion occurs.

A prototype taxi route conformance monitoring system is discussed in Brinton et al. [7], together with the operational concept, requirement, and procedure issues for practical implementations. In comparison, few direct references are found on algorithms of TOA taxi conformance monitoring. On the other hand, principles and methods developed for trajectory-based conformance monitoring in airborne operations may serve as useful references in the design of TOA taxi conformance monitoring algorithms. In particular, Reynolds and Hansman [8] pioneered the discussions of a trajectory conformance monitoring framework for commercial aircraft by applying model-based fault-detection techniques. Conformance residuals are defined as weighted sums of differences between the expected and observed aircraft state values. Seah et al. [9] further developed this approach by using a stochastic linear hybrid system model that can account for the random deviations of aircraft flight trajectories due to navigation uncertainties.

In addition, efforts have been made in developing methods for surface-trajectory prediction, which is a core component of taxi conformance monitoring. An example of surface-trajectory-based automation is the Surface Management System (SMS) [10], a decision support tool for airport surface scheduling and management that has been successfully used to improve the efficiency of surface operations [11]. SMS uses a surface-trajectory model based on constant speed and instantaneous acceleration to calculate taxi times to a specific airport resource such as a departure runway. These taxi times are then used to predict the schedules and sequences of aircraft arrivals at the runway. Controllers would use these predictions to assist them in managing demands for airport resources [12,13]. More advanced surface system concepts, such as taxi scheduling optimization, use constant-speed trajectory models to establish the initial schedules and sequences of aircraft not only at a runway, but also at a number of taxiway intersections along the route [3,4,14]. Since airport surface simulation tools are dependent on scheduling and sequencing predictions derived from surface-trajectory models, it is important to examine more realistic surface-trajectory models [15]. Recently, Gong [16] discussed methods of kinematic surface-trajectory predictions by analyzing actual traffic data from the Dallas–Fort Worth (DFW) airport. Wu et al. [17] examine different choices of surface-trajectory prediction models. Speed-profile constructions for estimating motion times have also been used in modeling automobile and ship movements [18–21].

This paper presents a systematic procedure and required algorithms for TOA taxi conformance monitoring for aircraft surface movements. In this paper, two methods of TOA predictions are first presented that form the basis of TOA taxi conformance monitoring: a dead-reckoning method and an intent modeling method. The dead-reckoning method assumes a constant speed for an aircraft from now to a specified checkpoint, whereas the intent modeling prediction incorporates likely variations of future aircraft speeds. Then a distance-varying conformance monitoring criterion is introduced that takes into consideration the aircraft's ability to achieve different TOA at the checkpoint starting from the current position, or its time controllability. Human-in-the-loop simulation traffic data from the DFW airport is used, and Monte Carlo simulations are conducted over likely uncertainties of aircraft state measurements to evaluate the proposed methods in terms of TOA prediction accuracy, speed-profile matching, and conformance prediction reliability.

II. Problem Statement

There are two essential time control points on the airport surface: gates and runway thresholds. In surface operations, individual aircraft may be sequenced and scheduled at these points, as well as some other critical points such as runway crossings. Because of uncertainties and different piloting styles, individual aircraft may transverse the airport at different paces, resulting in dispersions of arrival times at the runway thresholds or gates. This would require that margins be used in scheduling aircraft surface motions.

To help improve aircraft compliances with planned taxi schedules, a multiple-point time control concept may be used in which aircraft movements along a taxi route are tagged by a series of well-spaced traffic flow points, or checkpoints, between gates/spots and runway thresholds. An appropriate RTA can be defined for each checkpoint. Experimental evidences indicate that a larger number of checkpoints result in smaller TOA errors at the runways or gates [6]. This multiple-point time control scheme also has the advantage of ensuring sufficient separations among all aircraft on the surface. Figure 1 illustrates three checkpoints in a representative taxi route, where the last point is the runway threshold. In general, the selection of checkpoints and their corresponding RTA for a specific aircraft can depend on the airport configuration, the aircraft type, its performance capability, and airline procedures. Experimental results indicate that checkpoints should be located near salient flow points in order to achieve the most benefit, and pilot surveys favor two–three checkpoints per route [6].

This paper seeks to develop a systematic framework and necessary algorithms for TOA taxi conformance monitoring at a generic checkpoint. As shown in Fig. 2, such a TOA taxi conformance monitoring system predicts the likelihood that the aircraft shall meet the RTA at the specified checkpoint. In the event that the aircraft will likely be unable to meet the RTA, the taxi conformance monitoring system seeks to predict this nonconformance in the earliest possible time. Since the generic checkpoint can represent a runway threshold, a gate, or a traffic flow point in-between, the TOA taxi conformance monitoring methods of this paper are applicable to either a multiple-point time control scheme or surface automation systems that only schedule aircraft at runway thresholds and/or gates.

Actually, these methods may also be used to assist controllers in current surface operations to detect significant deviations of individual aircraft from historical traffic patterns. This requires a somewhat different interpretation of RTA. Specifically, if RTA at

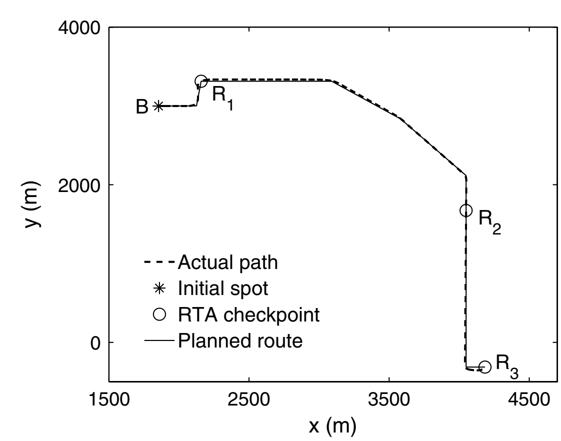

Fig. 1 Representative aircraft taxi route.

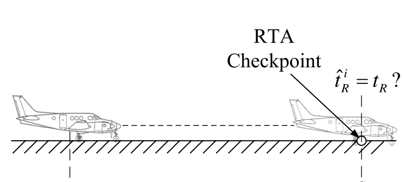

Fig. 2 Problem of TOA taxi conformance monitoring.

specified checkpoints are indeed issued to pilots as commands, the pilots would use closed-loop controls to achieve these RTA, and the name of RTA is appropriate. In the current surface operations, on the other hand, TOA at selected intermediate points during a taxi may not be scheduled or enforced, and thus may not be followed rigorously by the pilots. In this case, the RTA represent expected TOA at these intermediate points. These expected TOA can be obtained from historical traffic data in the airport of interest.

III. Overview of Solution Strategies

There are two crucial components in TOA taxi conformance monitoring: the prediction of TOA at checkpoints and the definition of a conformance criterion. Both have some unique challenges in taxi conformance monitoring compared with trajectory-based conformance monitoring for airborne operations.

To determine if an aircraft will conform to the RTA at a checkpoint, one needs to predict the likely TOA at the checkpoint based on the current information. TOA predictions depend not only on current aircraft states but also on future aircraft motion intents. In surface operations, an aircraft may use a combination of moves and stops, and can move at different speeds from the current position to the checkpoint. This can result in an infinite number of possible TOA at the checkpoint. Accordingly, an appropriate TOA prediction method needs to account for these possibilities.

In this paper, two different TOA prediction methods are presented: a dead-reckoning method and an intent modeling method. The dead-reckoning method assumes that the aircraft would maintain its current speed from now to the checkpoint. It is a straightforward method, but its predictions may not be accurate at all times. In comparison, the intent modeling method assumes a variable, dynamic speed profile for the aircraft from the current position to the checkpoint. Specifically, in this paper, the variable speed profile is modeled as a series of speed segments where in each segment, the aircraft may accelerate, decelerate, or maintain a constant speed. Both the number of segments in a speed profile and the magnitude of acceleration, deceleration, or constant speed in each segment can be selected to properly represent the likely motion intents of the aircraft. This method effectively introduces multiple parameters that can be turned to adapt to different characteristics of actual aircraft motion intents. It has the capability of making more accurate TOA predictions, at the expense of additional computations.

In addition, definitions of TOA taxi conformance criteria at specified checkpoints require some special attention. Intuitively, a simple conformance test on whether an aircraft will achieve the RTA at a checkpoint would be to compare a predicted TOA with the RTA at the checkpoint. If their difference exceeds a certain threshold, a nonconformance could be declared. However, there may be different possible ways to taxi the aircraft from the current position to the checkpoint. Accordingly, an effective conformance criterion should take into consideration the ability of the aircraft to alter its TOA before it actually arrives. For example, the predicted TOA at the checkpoint estimated at the current position may indicate a potential late arrival at the checkpoint. If the pilot realizes the time urgency and starts to speed up, the aircraft may still be able to arrive at the specified checkpoint on time. In other words, appropriate taxi conformance monitoring criteria should properly take into consideration pilot's ability to control the TOA at the checkpoint, or the time controllability.

In this paper, a conformance criterion is introduced as the ratio of the difference between the predicted TOA and the RTA at a checkpoint, over a measure of the aircraft time controllability at the current position that varies with the distance-to-go as well as aircraft performance capabilities.

IV. Time-of-Arrival Prediction via Dead-Reckoning

A straightforward method of predicting the TOA at a checkpoint is to assume that the aircraft shall maintain the current speed from now to the checkpoint. This method is called dead-reckoning. Specifically, based on the measured state information at the current time t_i, the distance-to-go from the current position to the RTA checkpoint can be determined as $s_R - \hat{s}_i$. The predicted TOA at the checkpoint can be calculated as

$$\hat{t}_R^i = t_i + \frac{s_R - \hat{s}_i}{\hat{V}_i} \tag{1}$$

This TOA prediction can be updated periodically when new surveillance information becomes available.

In general, surveillance measurements contain errors, and these errors will affect accuracies of the TOA predictions. In addition, the dead-reckoning formula may run into a singularity when $\hat{V}_i \approx 0$. To obtain meaningful solutions, aircraft performance bounds and typical operational constraints can be used to adjust the TOA predictions. In particular, feasible aircraft speeds during taxi may be bounded by some minimum speed $V_{\min}$ and maximum speed $V_{\max}$:

$$V_{\min} \leq \hat{V}_i \leq V_{\max} \tag{2}$$

An aircraft may stop on the taxi route. As a result, the minimum speed can be theoretically zero or $V_{\min} = 0$; making the predicted TOA infinitely large. This may be prevented by properly selecting $V_{\min}$ for dead-reckoning TOA predictions. In practical operations, an aircraft is expected to move on the taxi route at a reasonable average speed. Thus the minimum speed may be selected to reflect this average behavior. In this paper, it is assumed that $V_{\min} = 5$ kt and $V_{\max} = 33$ kt.

While simple, the dead-reckoning predictions do not consider the possibility of future speed changes. For intermediate checkpoints at which aircraft do not need to decelerate to a stop, dead-reckoning TOA predictions can be acceptable, especially if made at positions close to the specified checkpoint. For TOA predictions made at positions far from the checkpoint, on the other hand, the dead-reckoning predictions can potentially be erroneous.

V. Time-of-Arrival Prediction via Intent Modeling

More accurate TOA predictions may be made by considering possible aircraft motion intents from the current position to the checkpoint. However, this is challenging because the pilot may have many different ways of taxiing the aircraft before arriving at the checkpoint. This varying time controllability can result in an infinite number of possible TOA. In this paper, a variable-speed-profile structure is proposed that can represent different types of speed intents under normal operations.

A speed profile is defined as a series of individual speed segments from the current position to the checkpoint, where in each segment the aircraft may accelerate, maintain a constant speed, or decelerate. For simplicity, it is assumed that the aircraft would maintain a constant acceleration (deceleration) during an acceleration (deceleration) segment. Therefore, a quantitative definition of a speed profile first requires the specification of the number of distinct speed segments as well as locations on the taxi route at which one segment transitions into another. It then needs to specify the magnitudes of the speed, acceleration, or deceleration in each segment.

A. Speed-Profile Structure

Different possibilities in a single-segment profile and a two-segment profile are first examined. Speed profiles with larger number of segments can be obtained as combinations of these basic profiles.

A single-segment profile requires two parameters to describe: a discrete parameter for the speed type and a continuous parameter for the magnitude. Clearly, the dead-reckoning method is a special case of the single-segment profile in that it assumes a constant speed.

In a two-segment profile, there are 8 different possible combinations of speed types, as illustrated in Fig. 3. The case when two segments have the same constant speed is really a single segment and is thus omitted. In comparison, the case when an aircraft changes its speed from one constant value to another is a three-segment profile because of a required acceleration or deceleration segment in the middle. In Fig. 3, the circles in each drawing represent points where

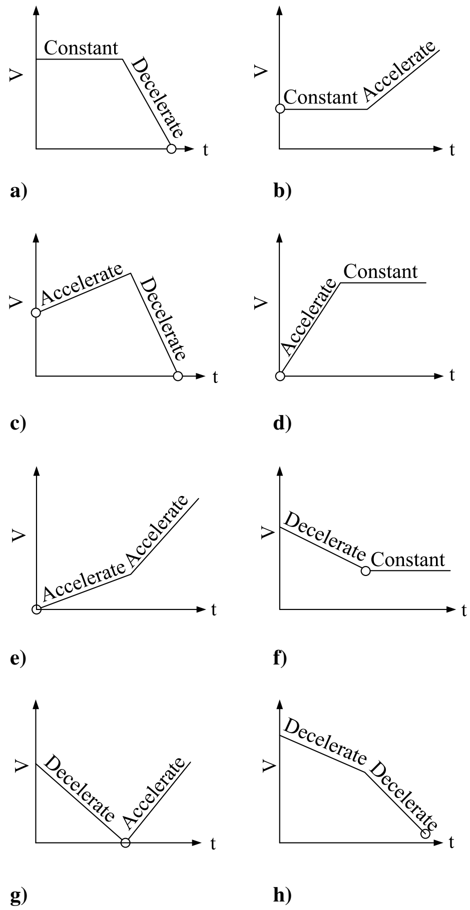

Fig. 3 Basic patterns of two-segment speed profiles.

the speed can be zero. In general, a two-segment speed profile requires four parameters to describe, which include the speed type as well as the magnitude for each segment.

As the number of segments increases further, the number of possible speed profiles increases drastically. For a three-segment structure, the number of independent speed profiles jumps to 22, and each speed profile requires six parameters to describe. In general, there are

$$\frac{(1+\sqrt{3})^{n+2}-(1-\sqrt{3})^{n+2}}{4\sqrt{3}}$$

distinct speed profiles for an n-segment structure [22], and each profile requires $2n$ parameters to quantify. Intuitively, the use of a larger number of speed segments makes it possible to more accurately describe aircraft motion intents over a longer taxi distance, but it also requires the specifications of more parameters that results in more complicated decision logics and a larger computational load.

B. Incorporation of Likely Aircraft Intents

To reduce the number of parameters in specifying a speed profile while maintaining its TOA prediction accuracy, characteristics of aircraft motion on different parts of a taxi route are now examined. Indeed, aircraft most likely follow certain speed trends over different parts of a taxi route in normal operations. Table 1 lists some heuristic rules for likely speed trends.

For example, when an aircraft begins its initial taxi, it would need to accelerate to gain some speed. As it approaches a middle checkpoint such as a cross section, it may slow down somewhat to check for other traffic but may not stop completely. It may also slow down when approaching a turn and then speed up somewhat after making the turn. Finally, as the aircraft approaches the last RTA checkpoint before entering the runway, it should slow down and may even stop.

These intent rules are not unique and may not apply at all times, but they can be used to reduce the number of segment possibilities in designing speed profiles for TOA predictions. In practical applications, past statistics at a given airport may be used to construct appropriate speed profiles. In addition, segment types and magnitudes in a speed profile can be adjusted adaptively in operations, when actual speed intents can be estimated from measurements.

To illustrate the construction of a speed intent profile, aircraft taxi from the initial spot B to the first RTA checkpoint R_1 in Fig. 4 is used as an example. The process is similar for other RTA checkpoints. For this part of the taxi route, the starting time at point B is t_0 and the RTA at checkpoint R_1 is t_R. The planned taxi route from B to R_1 consists of two legs, with a total distance of $d_1 + d_2$. At a generic time instant $t_i \in [t_0, t_R]$ during the taxi, the aircraft is at point C, where a surveillance measurement is made.

The rules in Table 1 are now applied to establish a speed profile for the intent modeling method. In addition to points B, C, and R_1, several additional characteristic points can be identified based on the geometry of the taxi route, at which an aircraft is likely to make speed changes. Point E and F represent the starting and ending point in a turn, whereas point G is close to the RTA checkpoint at which the aircraft will likely start to slow down. As a result, the aircraft speed profile during this part of the taxi may be divided into four smaller parts: $B \to E$, $E \to F$, $F \to G$, and $G \to R_1$. Each smaller part can be represented by a basic two-segment speed profile from Fig. 3, resulting in a total of eight speed segments. Using the heuristic rules in Table 1, a variable speed profile for TOA predictions at the RTA checkpoint R_1 can be established as shown in Fig. 5 and summarized in Table 2.

C. Estimation of Segment Magnitudes

To complete the definition of the speed intent profile, it is necessary to specify the magnitudes of speed, acceleration or deceleration for all individual segments in the profile. However, these magnitudes may not be unique, and there can be many possibilities even if the heuristic rules in Table 2 are applied. To further reduce the number of magnitude possibilities in the speed profile, a method is now proposed to estimate these magnitude intents based on characteristics of the speed-profile structure and the taxi route, as shown in Fig. 6.

Starting with the surveillance data at the current time t_i, the initial speed of the first segment is made equal to the current surveilled speed $\hat{V}_i$. If applicable, the initial acceleration (deceleration) is made equal to an estimated acceleration (deceleration) $\hat{\dot{V}}_i$ at the current position. This can typically be obtained by smoothing a few past surveillance data. To obtain a reliable estimate of the aircraft acceleration, the time interval over which past data are used should be comparable with the typical time constant of aircraft acceleration. For accelerations on the airport surface, this time constant is roughly 30 kt/0.1 g or about 15 s.

At the end of an acceleration segment, the aircraft is likely to use a larger speed than the commanded speed V_c. For TOA predictions, it may be assumed that the speed is V_c, $V_{\max}$ or somewhere in-between at $V^+ \in [V_c, V_{\max}]$. Similarly, at the end of a deceleration segment, the speed can be $V_{\min}$, V_c, or $V^- \in [V_{\min}, V_c]$. In this paper, the intermediate speed magnitudes are selected as

$$V^+ = \frac{V_{\max} + V_c}{2} \qquad V^- = \frac{V_{\min} + V_c}{2} \tag{3}$$

Table 1 Likely taxi speed trends in surface operations

Taxi position	Likely speed intent
Starting taxi	Accelerate
Approaching a turn	Decelerate but does not stop
After passing a turn	Accelerate somewhat
Approaching a mid-RTA checkpoint	Decelerate but does not stop
Approaching final RTA checkpoint	Decelerate to stop

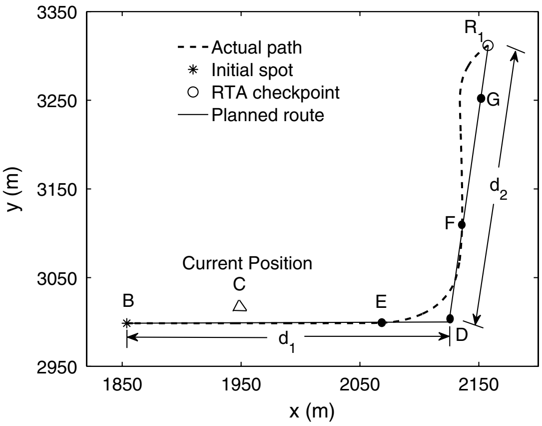

Fig. 4 Configuration of one segment.

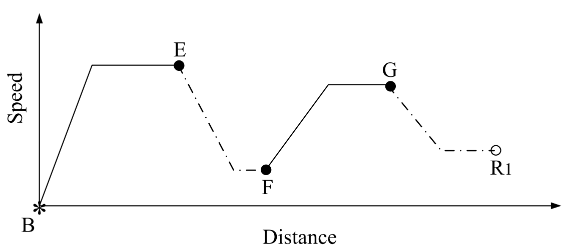

Fig. 5 TOA speed intent profile.

Once the magnitudes for the constant-speed segments are determined, the required acceleration or deceleration magnitudes for in-between segments can be calculated.

Selected speed and acceleration (deceleration) magnitudes should satisfy aircraft performance constraints. In addition to the speed constraints in Eq. (2), an aircraft also has constraints on its acceleration capability:

$$d_{\max} \leq \dot{V} \leq a_{\max} \tag{4}$$

Bounds on the speed and/or the acceleration need to reflect aircraft performance limitations, operational constraints, and/or typical operational practices. In this paper, the maximum acceleration and deceleration are assumed to be $a_{\max} = -d_{\max} = 0.1$ g.

If the resulting accelerations or decelerations based on assumed speed magnitudes exceed the aircraft performance limits in Eq. (4), the assumed speed magnitudes in Eq. (3) should be adjusted to satisfy these limits. Alternatively, magnitudes for the acceleration and deceleration segments may be specified, and the resulting speed magnitudes for the constant-speed segments can be determined accordingly.

D. Calculation of Time-of-Arrival Predictions

With an assumed speed intent profile, the predicted TOA at a checkpoint can be calculated, by integrating appropriate aircraft equations of motion. In actual taxi motions, an aircraft will likely deviate from the centerline of a taxi route. In estimating TOA, it can be assumed that aircraft move along the centerline with negligible lateral deviations. As a result, the distance along the centerline measured from the starting point becomes the only position coordinate, and $\dot{s} = V$:

Table 2 TOA speed intents for taxiing to checkpoint 1

Position	Motion Intent	Speed Intent	In Fig. 3
$B \rightarrow E$	Start taxi	Accel. to a speed	(d)
$E \rightarrow F$	Start a turn	Decel. to a nonzero speed	(f)
$F \rightarrow G$	End a turn	Accel. to a speed	(d)
$G \rightarrow R_1$	Approach checkpoint	Decel. to a speed	(f)

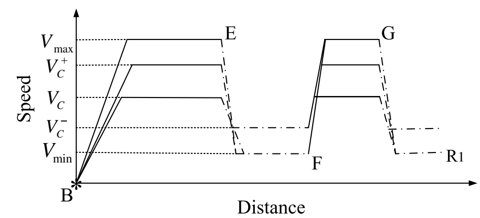

Fig. 6 Representative magnitudes of speed-profile intent models.

$$\frac{\mathrm{d}t}{\mathrm{d}s} = \frac{1}{V} \tag{5}$$

Given the initial position and the speed at the current position from surveillance, the TOA at the endpoint of a segment in a speed profile can be determined from

$$\hat{t}_R^j = t_i + \int_{\hat{s}_i}^{s_j} \frac{\mathrm{d}s}{\tilde{V}(s)} \tag{6}$$

where $\tilde{V}(s)$ is the variable speed function at the segment of integration. The predicted TOA at a checkpoint can be obtained by summing up transit times over individual segments.

VI. Design of Taxi Conformance Criteria

Once a TOA prediction is made for a specified checkpoint, conformance monitoring algorithms need to determine if the aircraft will likely be conforming to the RTA at that point. The difficulty of determining TOA conformances lies in the fact that the pilot still has many different ways of moving the aircraft from now to then. Therefore, an appropriate criterion for TOA taxi conformance monitoring should compare the difference between the predicted TOA and the RTA against the pilot's ability to alter the TOA, or time controllability.

A. Time Controllability

If the pilot realizes that it is going to be late, the pilot may accelerate the aircraft to reach a higher speed in an attempt to catch up. Constraints due to aircraft performance, airport regulations, and surface conditions may limit the maximum acceleration and/or the maximum speed that the aircraft can use. These limits effectively determine the shortest possible time that the aircraft needs to reach the checkpoint: $\hat{t}^i_{R\min}$. Conversely if the pilot realizes that it is going to be early, he/she may slow the aircraft down. The corresponding peak deceleration and the minimum feasible speed determine the longest time the aircraft can take to arrive at the checkpoint: $\hat{t}^i_{R\max}$. These two bounds define the range of time controllability at the current position: $[\hat{t}^i_{R\min}, \hat{t}^i_{R\max}]$. Because an aircraft can stop and wait on the taxi way, the maximum time bound can be considerably large. Still, the aircraft may not be able to stop and wait forever in normal operations because there are other aircraft behind.

In general, these time bounds depend on the distance-to-go, the aircraft's maximum acceleration and deceleration capabilities, and its feasible maximum and minimum speed. When the aircraft is still far away from a RTA checkpoint, the pilot usually has some flexibility in changing the speed intents to meet the RTA. As a result, the aircraft can still absorb a large difference between the RTA and the predicted TOA, and the time controllability is large. On the other hand, as the aircraft gets closer to the RTA checkpoint, the pilot's ability to control time decreases and the time controllability becomes smaller.

Figure 7 illustrates the speed profiles used in this paper in estimating the maximum and minimum feasible TOA at a RTA checkpoint. To arrive at the checkpoint in the shortest possible time, it is assumed that the pilot would increase the speed with a maximum acceleration level $a_{\max}$ to the maximum speed $V_{\max}$. Similarly, the latest possible TOA is estimated by assuming a speed reduction with the maximum deceleration $d_{\max}$ to the minimum feasible speed $V_{\min}$. Mathematically,

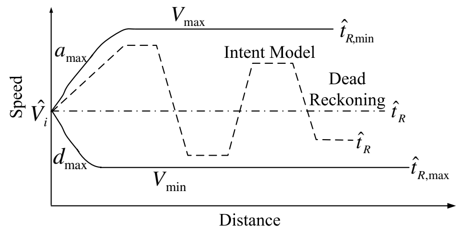

Fig. 7 Speed profile for minimum and maximum time.

$$
\hat{t}^i_{R\min} = \begin{cases} t_i + \frac{-\hat{V}_i + \sqrt{\hat{V}_i^2 + 2a_{\max}\Delta s^i_R}}{a_{\max}} & \Delta s^i_R < \Delta s^i_p \\ t_i + \frac{(V_{\max} - \hat{V}_i)^2}{2a_{\max}V_{\max}} + \frac{\Delta s^i_R}{V_{\max}} & \Delta s^i_R \geq \Delta s^i_p \end{cases}
$$

$$
\hat{t}^i_{R\max} = \begin{cases} t_i + \frac{-\hat{V}_i + \sqrt{\hat{V}_i^2 + 2d_{\max}\Delta s^i_R}}{d_{\max}} & \Delta s^i_R < \Delta s^i_p \\ t_i + \frac{(V_{\min} - \hat{V}_i)^2}{2d_{\max}V_{\min}} + \frac{\Delta s^i_R}{V_{\min}} & \Delta s^i_R \geq \Delta s^i_p \end{cases} \tag{7}
$$

where $\Delta s^i_R = s_R - \hat{s}_i$ is the estimated length of the taxi route from the current position to the RTA checkpoint and Δs^i_p is the length of the route required to accelerate or decelerate from $\hat{V}_i$ to $V_{\max}$ or $V_{\min}$ with the maximum acceleration or deceleration rate $a_{\max}$ or $d_{\max}$, respectively.

B. Conformance Metric

The likelihood whether the aircraft will conform to the RTA at the checkpoint may need to be evaluated by comparing the predicted TOA $\hat{t}^i_R$ and the RTA t_R, against the controllable time window at the current spot $[\hat{t}^i_{R\min}, \hat{t}^i_{R\max}]$. Figure 8 illustrates the different scenarios of TOA conformances. Below, a scalar conformance criterion is defined for the convenience of applications.

1) If $\hat{t}^i_{R\min} > t_R$, which implies that $\hat{t}^i_R > t_R$, the aircraft is predicted to be late (the top scenario in Fig. 8). In addition, it does not have sufficient time controllability to catch up. In this case, the aircraft will be nonconforming to the RTA at the checkpoint. A conformance criterion may be defined as

$$
I = \frac{\hat{t}^i_R - t_R}{\hat{t}^i_R - \hat{t}^i_{R\min}} \tag{8}
$$

where $I > 1$ corresponds to a late arrival nonconformance.

2) If $\hat{t}^i_{R\min} < t_R$ but $\hat{t}^i_R > t_R$, the aircraft is currently predicted to be late (the middle scenario in Fig. 8). However, it still has the ability to catch up. In other words, the aircraft may still be able to conform to the RTA if it speeds up. In this case, Eq. (8) is still applicable and it results in $0 < I < 1$, where the value of I is high.

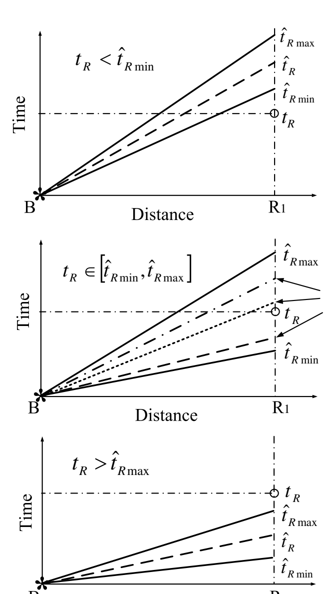

Fig. 8 Scenarios of RTA conformance.

3) If $\hat{t}^i_{R\min} < t_R$ and $\hat{t}^i_R > t_R$ but $\hat{t}^i_R \approx t_R$, the aircraft is predicted to be slightly late (also the middle scenario in Fig. 8). In this case, Eq. (8) is also applicable, with $0 < I < 1$ and I is small. The aircraft is conforming to the RTA if the predicted TOA is sufficiently close to the RTA.

4) If $\hat{t}^i_R < t_R$ and $\hat{t}^i_{R\max} > t_R$ but $\hat{t}^i_R \approx t_R$, the aircraft is predicted to be slightly early but is conforming to the RTA if the predicted TOA is sufficiently close to the RTA (also the middle scenario in Fig. 8). In this case, however, a new conformance criterion needs to be defined:

$$
I = \frac{\hat{t}^i_R - t_R}{\hat{t}^i_{R\max} - \hat{t}^i_R} \tag{9}
$$

where $-1 < I < 0$ and $|I|$ is small.

5) If $\hat{t}^i_R < t_R$ but $\hat{t}^i_{R\max} > t_R$, the aircraft is currently predicted to be early but it has the ability to absorb time (also the middle scenario in Fig. 8). In other words, the aircraft may still be able to conform to the RTA by slowing down. In this case, Eq. (9) is still applicable, and $-1 < I < 0$ where the value of $|I|$ is large.

6) Finally, if $\hat{t}^i_{R\max} < t_R$, which implies $\hat{t}^i_R < t_R$. The aircraft is projected to be too early and nonconforming (the lower scenario in Fig. 8). Equation (9) can also be used, which results in $I < -1$.

For use in practical operations, it is necessary to define a tolerance margin around the RTA: $\Delta t_R > 0$. As long as the aircraft arrives within $[t_R - \Delta t_R, t_R + \Delta t_R]$, it is considered to be conforming. A proper choice of Δt_R needs to balance the required pilot workload in controlling aircraft TOA and the system-wide scheduling efficiency for surface operations. To account for this tolerance margin as well as to avoid singularities in Eqs. (8) and (9) when $\hat{t}^i_R = \hat{t}^i_{R\min}$ or $\hat{t}^i_R = \hat{t}^i_{R\max}$, the above-defined conformance criteria are modified as follows:

$$
I = \begin{cases} \frac{\hat{t}^i_R - t_R}{\hat{t}^i_R - \hat{t}^i_{R\min} + \Delta t_R} & \hat{t}^i_R \geq t_R \\ \frac{\hat{t}^i_R - t_R}{\hat{t}^i_{R\max} - \hat{t}^i_R + \Delta t_R} & \hat{t}^i_R < t_R \end{cases} \tag{10}
$$

In this definition, the numerator is the difference between the RTA and the predicted TOA, or the predicted TOA error, whereas the denominator reflects the aircraft's current ability to achieve different TOA at the checkpoint. According to this definition, $I \geq 1$ represents a late arrival nonconformance whereas $I \leq -1$ represents an early arrival nonconformance. In comparison, $|I| < 1$ generally indicates that the aircraft still has the ability to conform to the RTA, where $I > 0$ means that the aircraft needs to speed up or it will be late, and $I < 0$ means that the aircraft needs to slow down or it will be too early. For $-\epsilon < I < \epsilon$, where $\epsilon > 0$ is some small number, the aircraft is projected to be conforming. Table 3 summarizes these different scenarios.

VII. Simulation Evaluations

Numerical simulations are now conducted to evaluate the performances of the proposed algorithms for TOA predictions and taxi conformance monitoring. Experimental traffic data from recent piloted simulations of time-based taxi clearances conducted by NASA researchers [6] are used for comparison with the simulation results. Three performance criteria are used in the evaluations. They are the accuracy of TOA predictions, qualitative matching of the speed profiles, and the reliability of conformance predictions.

Figure 9 shows the layout of the DFW airport, where a representative taxi route is illustrated. An enlarged version of this route is shown in Fig. 1. In the experiment, the pilots are provided with a series of three checkpoints, their associated RTA, and speed commands between these checkpoints [6]. Figure 10 plots the speed profiles and the RTA commands for these traffic data, where the top plot compares the commanded and measured speed profiles, and the lower plot shows the three RTA commands at the three different checkpoints. The measured speeds exhibit considerable variations

Table 3 Conformance scenarios

Scenario	Conditions	Metric value	Conformance status
1	$\hat{t}_{R\min} \geq t_R + \Delta t_R$	$I \geq 1$	Late nonconformance
2	$\hat{t}_{R\min} < t_R + \Delta t_R$	$\epsilon < I \leq 1$	Potential late nonconformance
2	$\hat{t}_R > t_R + \Delta t_R$	——	Aircraft can still speed up
3	$t_R \leq \hat{t}_R \leq t_R + \Delta t_R$	$0 < I < \epsilon$	Likely conformance
4	$t_R - \Delta t_R \leq \hat{t}_R < t_R$	$-\epsilon < I < 0$	Likely conformance
5	$\hat{t}_{R\max} > t_R - \Delta t_R$	$-1 \leq I < -\epsilon$	Potential early nonconformance
5	$\hat{t}_R < t_R - \Delta t_R$	——	Aircraft can still slow down
6	$\hat{t}_{R\max} \leq t_R - \Delta t_R$	$I \leq -1$	Early nonconformance

around the commanded speeds. This is in part caused by the fact that the pilot needs to adjust instantaneous speeds according to the taxi route conditions in controlling the aircraft. It may also be caused by surveillance errors.

Algorithms for TOA predictions and conformance monitoring are similar for each RTA checkpoint, so that only one RTA checkpoint is selected as an example. The first part of the aircraft taxi from the beginning point B to the first RTA checkpoint exhibits the most fluctuations in the actual speed history and may be the most interesting checkpoint to examine. It is therefore used in the numerical studies. The real data for this part provide that the commanded speed is $V_c = 18$ kt, the commanded RTA is $t_R = 88.39$ s, and the measured TOA is $\bar{t}_R = 95.72$ s.

Table 4 gives locations of the internal points for this part of the taxi route that correspond to the speed intent profile in Fig. 6. Throughout the simulations, we assume that the distance parameters specified in Table 4 are fixed. For the initial segment. the acceleration value is obtained by averaging the measured speeds in the previous 15 s. To implement the speed intent profile in Fig. 6, two sets of intent speed magnitudes are defined in an effort to examine their effects on the TOA prediction accuracy and the conformance prediction reliability.

Intent model 1:

$$V_E = V_c, \qquad V_F = V^-, \qquad V_G = V_{\max}, \qquad V_{R_1} = V^-$$

Intent model 2:

$$V_E = V_{\max}, \qquad V_F = V^-, \qquad V_G = V_c, \qquad V_{R_1} = V^-$$

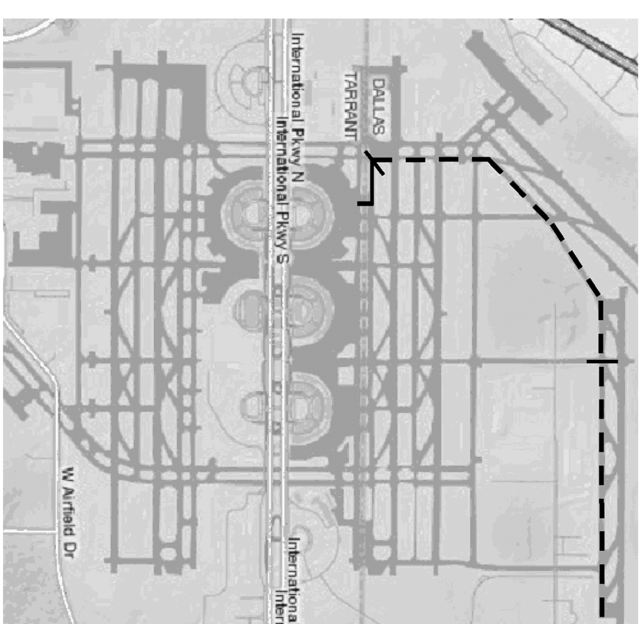

Fig. 9 Layout of the DFW airport and a representative taxi route.

VIII. Numerical Results

Numerical results are now presented. It is assumed that the algorithms for TOA predictions and taxi conformance monitoring are updated every 5 s, and $\Delta t_R = 8$ s.

A. TOA Prediction Errors

Figure 11 compares the mean histories of predicted TOA at a series of taxi positions before reaching the RTA checkpoint, obtained with the dead-reckoning method and intent model 1, respectively. TOA prediction errors are defined as $\hat{t}_R - t_R$ so that a positive value indicates a likely late arrival and a negative value an early arrival. Prediction starts when the time is 61 s ahead of the RTA checkpoint. With the dead-reckoning method, the predicted TOA error is generally large when the aircraft is far away from the RTA checkpoint but it improves as the aircraft gets closer to the checkpoint. In comparison, TOA predictions by the intent modeling method are consistently closer to the actual TOA.

To understand the performances of the proposed algorithms in the presence of likely surveillance errors, Monte Carlo simulations are conducted. In this paper, the simulated speed measurement errors are assumed to be normally distributed with a zero mean and a standard deviation of $\frac{8}{3}$ kt. A total of 100 simulations are run at each prediction update. Figure 12 presents the 95 percentile contours of predicted TOA error variations caused by speed measurement errors. It shows that the intent modeling method can provide more reliable TOA predictions in the presence of measurement errors than the dead-reckoning method, in addition to providing more accurate mean TOA predictions.

To examine the effects of different speed magnitudes on TOA predictions, intent model 2 is also studied. Figure 13 shows the mean predicted TOA errors using the three TOA prediction models: dead-reckoning, intent model 1, and intent model 2. intent model 2 does not predict the TOA as well as intent model 1, but it still performs better than the dead-reckoning method, especially at the beginning, when the aircraft speed is small. On the other hand, the three models produce essentially the same results when the aircraft gets close to the RTA checkpoint.

B. Speed-Profile Matching

In Figs. 14–17, the actual speed curves represent the NASA experiment data that were obtained with nonconstant sampling rates ranging from 0.03 to 0.06 s. When the conformance monitoring system is used, it is expected that the surveillance cycle would vary between 1 to 5 s. In the current study, the measured speeds are extracted from the experiment speed data with a sampling rate of 5 s. These speed values also serve as the nominal surveilled speeds in the Monte Carlo simulations.

Figure 14 shows the periodically updated speed profiles (every 5 s) obtained by the dead-reckoning method at a series of taxi positions before arriving at the RTA checkpoint. As expected, these speed profiles are constant lines at the measured speeds. In comparison, Fig. 15 shows the periodically updated speed profiles obtained by the intent modeling method at a series of taxi positions before arriving at the RTA checkpoint. Qualitatively, the intent modeling method can match the actual speed profile much better than the dead-reckoning method.

Table 4 Intent model parameters

Position	Intent structure	Intent magnitudes
Before E	Accelerates with a_E and then stays at V_E	Distance $\lvert ED \rvert = 170$ m a_E $V_E = V_c$, V^+, or $V_{\max}$
E to F	Decelerates with a_F and then stays at V_F	Distance $\lvert DF \rvert = 50$ m a_F $V_F = V^-$ or $V_{\min}$
F to G	Accelerates with a_G and then stays at V_G	Distance $\lvert GR_1 \rvert = 120$ m a_G $V_G = V_c$, V^+, or $V_{\max}$
G to R_1	Decelerates with a_{R_1} and then stays at V_{R_1}	a_{R_1} $V_{R_1} = V^-$ or $V_{\min}$

Figure 16 shows variations of predicted speed profiles using the intent modeling method when potential speed measurement errors are present at each update. It shows that the qualitative match between actual and modeled speed intents can deteriorate in the presence of surveillance errors, but the variable-speed-profile structure of the intent modeling method is still more capable of matching the actual speed profile than the dead-reckoning method.

Figure 17 shows the predicted speed profiles using intent model 2. In this case, speed magnitudes in intent model 2 do not closely represent the actual speed magnitudes; causing a little mismatch between the actual speed profile and intent model 2. This suggests that proper selections of the segment magnitudes in the intent modeling method are important. Still, the resulting TOA predictions by intent model 2 are overall better than those by the dead-reckoning method, as shown in Fig. 13.

C. Conformance Monitoring Reliability

Figure 18 shows the histories of the taxi conformance metric in Eq. (10) calculated at different update positions on the taxi route as the aircraft proceeds to the RTA checkpoint. The solid circle line represents the actual conformance metric, which is computed by replacing the predicted TOA $\hat{t}_R^i$ in Eq. (10) by the actual TOA. In this example, the actual TOA differs from the RTA by 7.33 s that is within $\Delta t_R = 8$ s. This indicates that the aircraft conforms to the RTA but arrives a little late. Accordingly, the conformance metric curve is consistently above the zero line. The metric calculated with TOA predictions by the dead-reckoning method displays fairly substantial deviations from the actual metric. In particular, the dead-reckoning method produces a large conformance metric value at the beginning due to the small initial speed. This increases the likelihood of reporting a nonconformance when in reality the aircraft is conforming to the RTA. In comparison, the intent modeling method effectively avoids the wrong inference at the beginning, and the two intent models display smaller deviations. Between the two, intent model 2 shows a larger deviation from the actual metric, as expected. This suggests that a reliable TOA prediction is essential in predicting the aircraft conformance status.

Monte Carlo simulations are again used to illustrate the variations of the taxi conformance metric that can be caused by potential

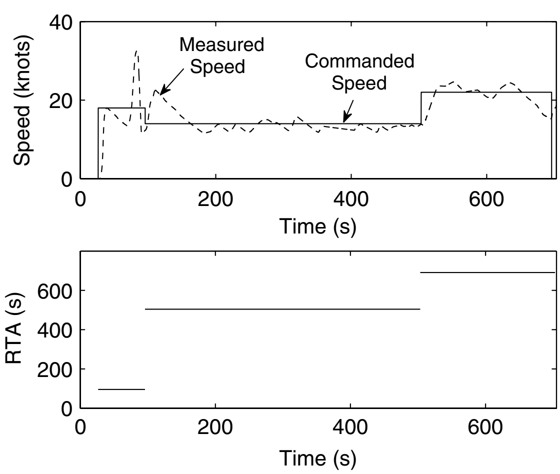

Fig. 10 Speed profile and accumulative RTA.

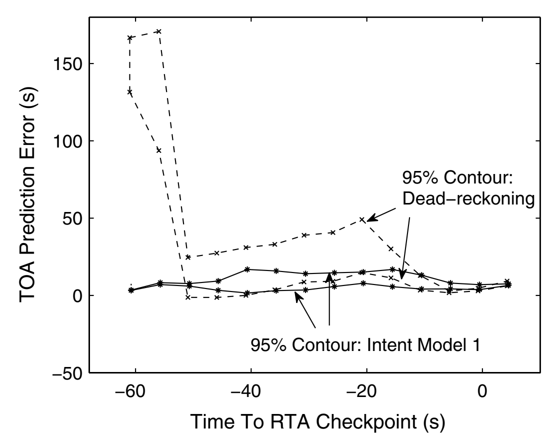

Fig. 12 Monte Carlo simulations of predicted TOA errors with surveillance uncertainties.

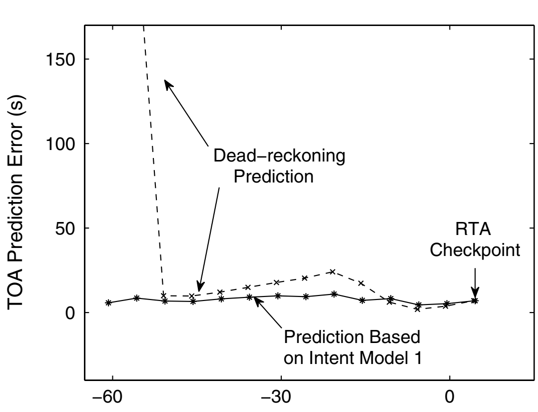

Fig. 11 Mean predicted TOA errors using dead-reckoning and intent model 1.

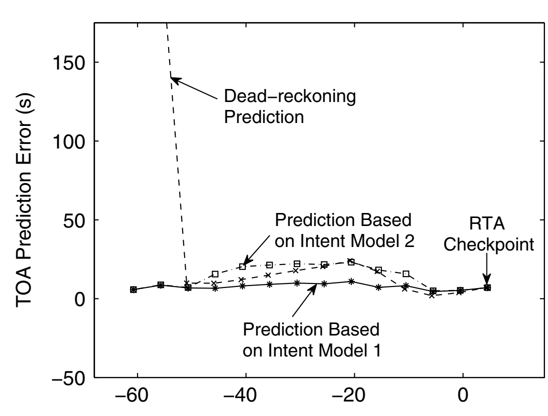

Fig. 13 Mean predicted TOA errors using dead-reckoning and intent models.

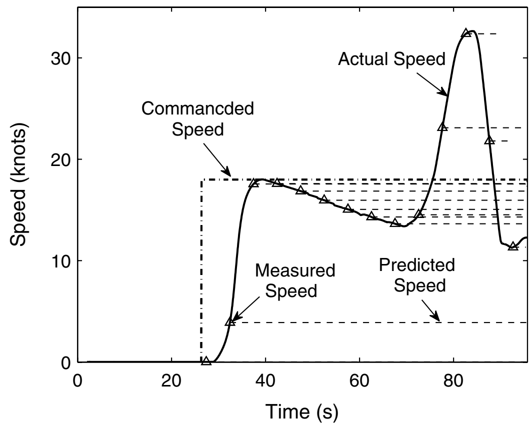

Fig. 14 Predicted speed profile using the dead-reckoning method.

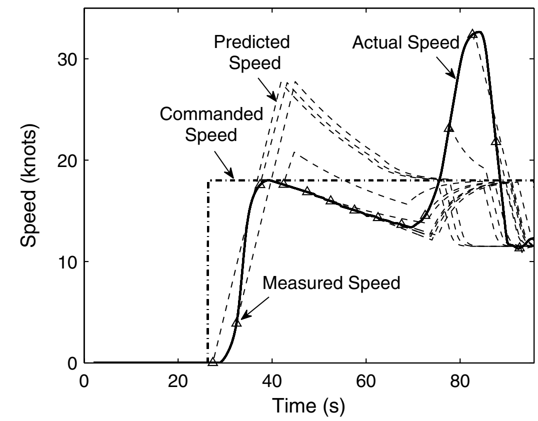

Fig. 17 Predicted speed profiles using intent model 2.

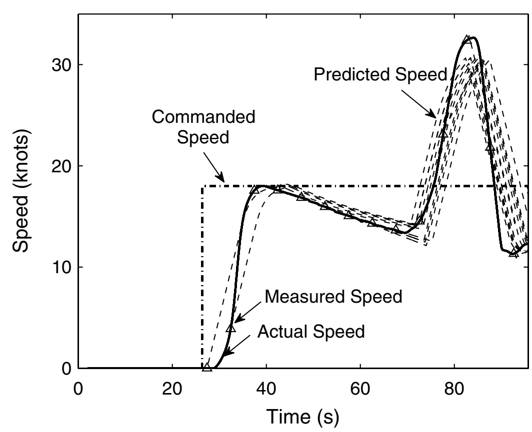

Fig. 15 Predicted speed profile using intent model 1.

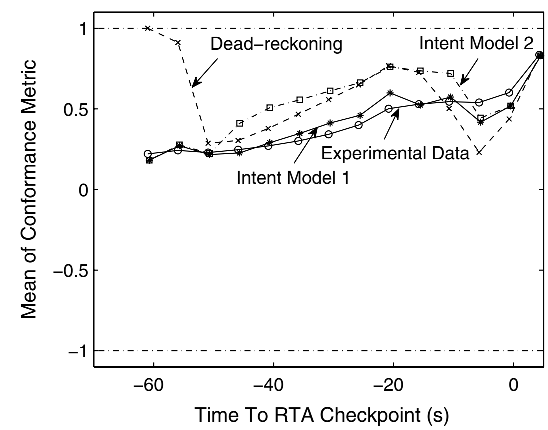

Fig. 18 Histories of taxi conformance metric using dead-reckoning and intent models.

surveillance errors. Figure 19 presents the 95 percentile contours of the conformance metric values for the three intent models. It shows that the ranges of conformance metric variations are smaller with the two intent models than that with the dead-reckoning method. In other words, the intent modeling method with its variable speed profile can provide more reliable predictions of the conformance status than the dead-reckoning method.

D. Speed Profile with a Stopping Segment

TOA nonconformance can be caused by aircraft stoppages during taxi, due to the presence of other aircraft in the path or at checkpoints. The intent modeling method can include stoppage segments in its speed profile to account for these possibilities, where the stopping position and the length of the stop become model parameters. In comparison, the dead-reckoning method would produce significantly worse predictions when a stopping segment is present.

As an example, it is assumed that the aircraft stops at the checkpoint R_1 for 5 s before proceeding further. Three additional speed segments are added to the intent model 1 speed profile discussed above: a deceleration-to-zero segment, a stop segment, and an acceleration segment, as shown in Fig. 20. It is assumed that the aircraft reduces its speed using maximum deceleration before

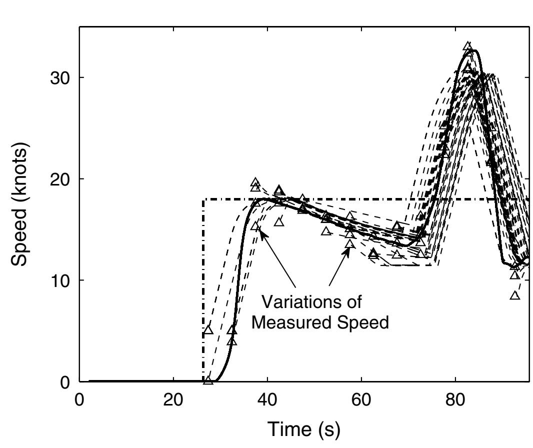

Fig. 16 Monte Carlo simulations of predicted speed profiles using intent model 1.

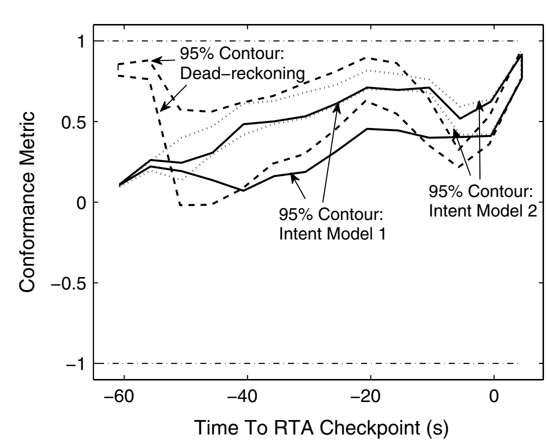

Fig. 19 Contours of conformance metrics using dead-reckoning and intent models.

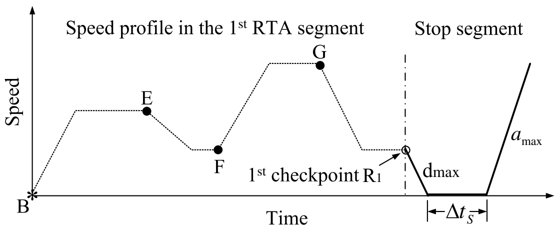

Fig. 20 Speed structure with a stop segment.

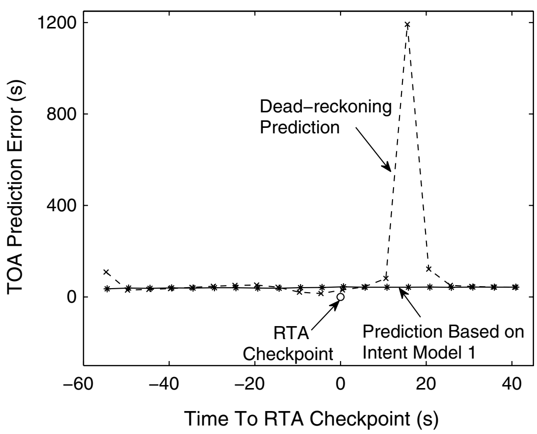

Fig. 21 Mean predicted TOA errors using dead-reckoning and intent models.

arriving at the stop segment and accelerates with maximum acceleration afterwards.

Figure 21 compares the average TOA predictions by the dead-reckoning method and the intent modeling method. Because of the zero speed, the dead-reckoning method results in a sharp increase in the predicted TOA at the stop segment. In comparison, the intent modeling method gives much more reasonable TOA predictions. Figure 22 shows the conformance metrics for the two methods. With the dead-reckoning method, the conformance metric varies considerably during the stop segment. This would produce false alarms. In comparison, the intent modeling method consistently produces accurate and reliable conformance predictions. In other words, the intent modeling method shows a significant superiority over the dead-reckoning method in terms of predicted TOA accuracies and conformance prediction reliability when there is a stop segment.

E. Discussions

The above results indicate that the intent modeling method performs better than the dead-reckoning method, in terms of TOA prediction accuracy, speed-profile matching, and conformance prediction reliability. Qualities of the intent modeling method do deteriorate somewhat if magnitudes of the speed segments are not properly selected. Still, the initial predicted TOA errors using either of the two intent models are much smaller than that using the dead-reckoning method. In addition, the intent modeling method is significantly superior than the dead-reckoning method when the actual speed profile contains stoppages during taxi.

Actually, the dead-reckoning method can be considered a special case of the intent modeling method, in which there is only one segment with a constant speed. In general, the intent modeling method introduces a variable structure for the speed profile that can include a number of different segments for accurately modeling different types and variations of actual aircraft intents. As a result, the intent modeling method provides a highly flexible framework with a continuum of varying speed profiles for accurate TOA predictions and reliable conformance monitoring.

Research efforts are underway to develop a stochastic framework that can potentially lead to performance improvements of conformance monitoring. In such a framework, variations of speed magnitudes in a given speed profile under likely surveillance uncertainties are taken into consideration. The statistical distribution of the resulting conformance metrics is used to estimate the probability of conformance, which would replace the deterministic conformance metric in this paper. Results shall be reported later.

Future work shall study intelligent methods for the automatic determination of speed profiles and the corresponding speed magnitudes. When little information is available on actual aircraft intents, one can simply assume a single speed segment with a constant speed. The dead-reckoning method results. The constant-speed magnitude can be determined initially from surveillance data. As more information is known about the natures of the taxi route, aircraft performance capabilities, likely aircraft motion characteristics, and/or future intents, the speed profile can be expanded to include additional segments for more accurate TOA predictions at various checkpoints. Likely magnitudes of speeds and/or accelerations in these segments can be estimated from this information, as well as from past traffic data. An adaptive scheme may even be developed to improve the intent speed profile in real time. Future research shall also examine the sensitivities of TOA prediction accuracies and conformance prediction reliabilities to variations in the number and magnitudes of the speed profile, and shall consider different ways of estimating the time controllability ranges.

Finally, a nonconformance at a checkpoint can potentially have a cascading effect on the subsequent checkpoints unless some corrective measures are taken. In an integrated solution for surface operations, a nonconformance information during one route segment can be incorporated into the system-wide scheduling algorithms, so that new trajectory commands are obtained at the beginning of the subsequent segment. As a result, the nonconformance in the previous segment can be cancelled out. Studies are needed on the integration of multiple-aircraft scheduling and individual aircraft conformance monitoring.

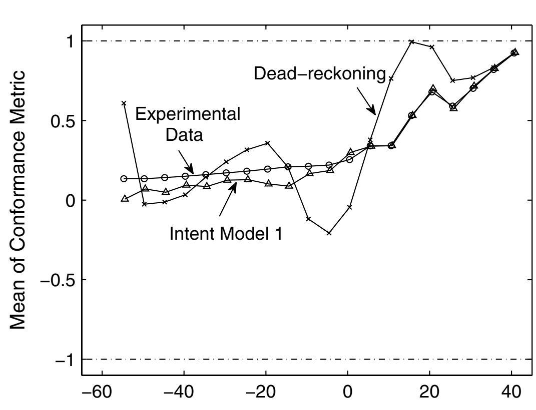

Fig. 22 Histories of taxi conformance metric using dead-reckoning and intent models.

IX. Conclusions

A systematic framework for time-of-arrival (TOA) aircraft taxi conformance monitoring in surface operations is developed. It is based on predicting the TOA at a checkpoint on the taxi route and properly comparing the predicted TOA with the required TOA (RTA) at the checkpoint. In this paper, two TOA prediction methods are first examined: a dead-reckoning method and an intent modeling method. The dead-reckoning prediction assumes a constant speed for the aircraft from the current position to the RTA checkpoint, whereas the intent modeling method assumes a variable speed profile with a series of different segments to imitate likely aircraft motion intents in the near future. Definition of a speed intent profile requires the specification of the number of distinct segments, locations at which one segment transitions into another, and magnitudes of the speed, acceleration, or deceleration in all the segments. In this paper, geometric conditions of the taxi route and aircraft performance capabilities are used to select the number of profile segments as well as the magnitudes.

Next, a conformance monitoring metric is introduced to assess an aircraft's ability to meet the RTA at a checkpoint. This conformance metric is devised to explicitly account for the aircraft's ability in achieving different TOA at the checkpoint or its time controllability. It is defined as the ratio of the TOA prediction error over the available time controllability estimated at the current position. In essence, this conformance metric combines information of current measurements of aircraft state, its speed and acceleration limits, its distance to the target, and likely future speed variations.

Numerical simulations are used to evaluate the performances of the proposed framework and algorithms in comparison with experimental data from the Dallas–Fort Worth (DFW) airport. In particular, Monte Carlo simulations are conducted over likely surveillance errors. Three criteria are used in these evaluations: TOA prediction accuracy, qualitative speed-profile matching, and conformance prediction reliability. Overall, the intent modeling method performs better than the dead-reckoning method in all three categories, which is nonetheless simpler to use.

Actually, the dead-reckoning method can be viewed as a special case of the intent modeling method in that there is only one segment in the speed profile. As a result, the intent modeling method in general provides a continuum of intent structures with a varying number of different speed segments. A larger number of segments in the profile can potentially lead to more accurate TOA predictions, better speed-profile matching, and more reliable conformance predictions, at the expense of the need to select more model parameters.

Acknowledgments

This research was supported by NASA under NASA Research Announcement contract NNA09DA89C to Mosaic ATM, Inc., with the University of Minnesota as a subcontractor. We thank David Foyle for providing access to the experimental data used in their studies and Yoon Jung for helpful discussions. We also thank anonymous reviewers for correcting a factual error and for many helpful suggestions.

References

[1] "Next Generation Air Transportation System: Integrated Plan," 2004, Joint Planning and Development Office, http://www.jpdo.gov/library/NGATS_v1_1204r.pdf, [retrieved 30 June 2008].

[2] Jung, Y. C., and Monroe, G. A., "Development of Surface Management System Integrated with CTAS Arrival Tool," AIAA 5th Aviation Technology, Integration, and Operations (ATIO) Conference, Arlington, VA, AIAA Paper 2005-7334, Sept. 2005.

[3] Balakrishnan, H., and Jung, Y., "A Framework for Coordinated Surface Operations Planning at Dallas–Fort Worth International Airport," AIAA Guidance, Navigation, and Control Conference, Hilton Head, SC, AIAA Paper 2007-6553, Aug. 2007.

[4] Rathinam, S., Montoya, J., and Jung, Y., "An Optimization Model for Reducing Aircraft Taxi Times at the Dallas Fort Worth International Airport," *26th International Congress of the Aeronautical Sciences (ICAS)*, Anchorage, AK, Sept. 2008.

[5] Williams, J. L., Hooey, B. L., and Foyle, D. C., "4-D Taxi Clearances: Pilots' Usage of Time- and Speed-Based Formats," AIAA Modeling and Simulation Technologies Conference, Keystone, CO, AIAA Paper 2006-6611, Aug. 2006.

[6] Foyle, D. C., Hooey, B. L., Kunkle, C. L., Schwirzke, M. F. J., and Bakowski, D. L., "Piloted Simulation of NextGen Time-Based Taxi Clearances and Tailored Departures," *Proceedings of the 2009 IEEE/AIAA Integrated Communications, Navigation and Surveillance Conference (ICNS)*, Arlington, VA, May 2009, pp. 1–11.

[7] Brinton, C. R., Atkins, S. C., and Hall, A., "Analysis of Taxi Conformance Monitoring Algorithms and Performance," *Proceedings of the Integrated Communication, Navigation and Surveillance Conference (ICNS)*, 2007.

[8] Reynolds, T. G., and Hansman, R. J., "Investigating Conformance Monitoring Issues in Air Traffic Control Using Fault Detection Techniques," *Journal of Aircraft*, Vol. 42, No. 5, 2005, pp. 1307–1317. doi:10.2514/1.10055

[9] Seah, C. E., Aligawesa, A., and Hwang, I., "An Algorithm for Conformance Monitoring in Air Traffic Control," AIAA Guidance, Navigation, and Control Conference, Chicago, IL, AIAA Paper 2009-6170, Aug. 2009.

[10] Atkins, S., Jung, Y., Brinton, C., Stell, L., Carniol, T., and Rogowski, S., "Surface Management Field Trial Results," 4th Aviation Technology, Integration, and Operations (ATIO) Forum, AIAA Paper 2004-6241, Sept. 2004.

[11] Atkins, S., Brinton, C., Waltion, D., Arkind, K., and Moertl, P., "Results from the Initial Surface Management System Field Tests," *5th Eurocontrol/FAA ATM RD Seminar*, 2003.

[12] Cheng, V. H., "Airport Surface Operation Collaborative Automation Concept," *Proceedings of the AIAA Guidance, Navigation, and Control Conference*, AIAA Paper 2003-5773, 2003.

[13] Cheng, V., Sharma, V., and Foyle, D., "A Study of Aircraft Taxi Performance for Enhancing Airport Surface Traffic Control," *IEEE Transactions on Intelligent Transportation Systems*, Vol. 2, No. 2, June 2001, pp. 39–54. doi:10.1109/6979.928715

[14] Atkins, S., Brinton, C., and Jung, Y., "Implications of Variability in Airport Surface Operations on 4-D Trajectory Planning," AIAA Aviation Technology, Integration, and Operations (ATIO) Conference, AIAA Paper 2008-8960, Sept. 2008.

[15] Swenson, H., Hoang, T., Engelland, S., Vincent, D., Sanders, T., Sanford, B., and Heere, H., "Design and Operational Evaluation of the Traffic Management Advisor at the Fort Worth Air Route Traffic Control Center," *1st USA/Europe ATM RD Seminar*, 1997.

[16] Gong, C., "Kinematic Airport Surface Trajectory Model Development," AIAA Aviation Technology, Integration, and Operations Conference (ATIO), AIAA Paper 2009-7076, Sept. 2009.

[17] Wu, D., Zhao, Y. J., and Capozzi, B. J., "Fundamental Models of Surface Trajectory Prediction for Advanced Air Traffic Management," AIAA 10th Aviation Technology, Integration, and Operations (ATIO) Technical Forum, Fort Worth, TX, AIAA Paper 2010-9009, Sept. 2010.

[18] Barbosa, M. H., Tight, R. M., and May, D. A., "A Model of Speed Profiles for Traffic Calmed Roads," *Transportation Research, Part A (Policy and Practice)*, Vol. 34, No. 2, 2000, pp. 103–123. doi:10.1016/S0965-8564(98)00067-6

[19] Collins, M. K., and Krammes, A. R., "Preliminary Validation of a Speed-Profile Model for Design Consistency Evaluation," *Transportation Research Record*, Vol. 1523, 1996, pp. 11–21. doi:10.3141/1523-02

[20] Hellstrom, T., "Optimal Pitch, Speed and Fuel Control at Sea," *Journal of Marine Science and Technology*, Vol. 12, No. 2, 2004, pp. 71–77.

[21] Taylor, R. D., Muthiah, S., Kulakowski, T. B., Mahoney, M. K., and Porter, J. R., "Artificial Neural Network Speed Profile Model for Construction Work Zones on High-Speed Highways," *Journal of Transportation Engineering*, Vol. 133, No. 3, 2007, pp. 198–204. doi:10.1061/(ASCE)0733-947X(2007)133:3(198)

[22] Sloane, N. J. A., *On-Line Encyclopedia of Integer Sequences*, Item A028859, http://www.research.att.com/njas/sequences/.